The Journal of Experimental Biology 208, 2177-2190
Published by The Company of Biologists 2005
doi:10.1242/jeb.01615

CCA-1, EGL-19 and EXP-2 currents shape action potentials in the *Caenorhabditis elegans* pharynx

Boris Shtonda* and Leon Avery

Department of Molecular Biology, University of Texas Southwestern Medical Center, 6000 Harry Hines Blvd., Dallas, TX 75390-9148, USA

*Author for correspondence (e-mail: boris@eatworms.swmed.edu)

Accepted 19 February 2005

Summary

The pharynx of *Caenorhabditis elegans* is a tubular muscle controlled by its own set of neurons. We developed a technique to voltage clamp the pharyngeal muscle and demonstrate by analyzing mutants that the pharyngeal action potential is regulated by three major voltage-gated currents, conducted by a T-type calcium channel CCA-1, an L-type calcium channel EGL-19 and a potassium channel EXP-2.

We show that CCA-1 exhibits T-type calcium channel properties: activation at –40 mV and rapid inactivation. Our results suggest that CCA-1's role is to accelerate the action potential upstroke in the pharyngeal muscle in response to excitatory inputs. Similarly to other L-type channels, EGL-19 activates at high voltages and inactivates slowly; thus it may maintain the plateau phase of the action potential. EXP-2 is a potassium channel of the kV family that shows inward rectifier properties when expressed in *Xenopus laevis* oocytes. We show that endogenous EXP-2 is not a true inward rectifier – it conducts large outward currents at potentials up to +20 mV and is therefore well suited to trigger rapid repolarization at the end of the action potential plateau phase. Our results suggest that EXP-2 is a potassium channel with unusual properties that uses a hyperpolarization threshold to activate a regenerative hyperpolarizing current.

Key words: calcium channel, L-type/T-type/potassium channel, *Caenorhabditis elegans.*

Introduction

In *Caenorhabditis elegans* the pharynx is the feeding organ. It has been utilized previously as a versatile system to study how genes control excitability and behavior (Avery, 1993a; Avery and Horvitz, 1989). During pharyngeal contractions (each contraction/relaxation cycle is called a pump), soil bacteria are sucked in, trapped, ground and transported to the intestine, while the liquid is spat out (Doncaster, 1962; Seymour et al., 1983). The anatomy of the pharynx has been reconstructed from serial section electron micrographs (Albertson and Thomson, 1976). The pharynx contains 20 muscle cells, seven marginal cells, nine epithelial cells, four gland cells and 20 neurons. In the pharyngeal nervous system, two types of paired motor neurons are most relevant to our work: MC and M3. MC neurons synapse on mc2 marginal cells (Albertson and Thomson, 1976) and probably pm4 muscle cells (L.A., unpublished observations) to excite the pharyngeal muscle *via* the EAT-2/EAT-18 acetylcholine receptor, making it pump rapidly (McKay et al., 2004; Raizen et al., 1995). The pharyngeal muscle also has an MC-independent, presumably myogenic, mechanism of generating action potentials; so that worms in which MC function is abolished are still *via*ble, although the pharyngeal pumping rate is reduced from 200 per minute to about 50. Even after the whole pharyngeal nervous system is killed, pumping still continues at a low rate (Avery and Horvitz, 1989). Another pharyngeal neuron, M3, contributes to the repolarization by causing small notch hyperpolarizations (IPSPs) during contraction (Raizen and Avery, 1994); it signals to the pharyngeal muscle *via* a glutamate-gated chloride channel AVR-15 (Dent et al., 1997).

To observe the electrical activity of the pharynx, Raizen and Avery (1994) invented pharyngeal extracellular recordings – electropharyngeograms – and Davis and Avery (Davis, 1995) developed sharp electrode voltage recording from the pharyngeal muscle. Methods for voltage clamp recordings on *C. elegans* neurons (Goodman et al., 1998) and body wall muscle (Richmond and Jorgensen, 1999) have also been established. Using these preparations, a variety of ligand and voltage-gated channels have been studied (Francis et al., 2003; Jospin et al., 2002a,b; Mellem et al., 2002; Pierce-Shimomura et al., 2001). In this study, we develop a voltage clamp technique for the *C. elegans* pharynx and look at the *in vivo* function of pharyngeal ion channels.

The following model for the pharyngeal muscle is best supported by the previous work. MC fires, causing an excitatory post-synaptic potential (EPSP), which activates the EGL-19 L-type calcium channel (Lee et al., 1997). Calcium

entry through EGL-19 further depolarizes the pharynx and causes contraction. During contraction, M3 fires, causing small notch hyperpolarizations (IPSPs). At some point, possibly triggered by M3 IPSPs, the potassium channel EXP-2 recovers from inactivation, causing a full rapid repolarization (Davis et al., 1999). Here we show, using the voltage clamp, that this model is generally correct with respect to EGL-19 and EXP-2, but that one player, a T-type calcium channel CCA-1, had been overlooked. In the pharyngeal muscle, CCA-1 mediates a large inward depolarizing current, which is the first demonstrated role of the T-type calcium channel in *C. elegans.* This finding, along with the accompanying work (Steger et al., 2005), suggest that CCA-1 activates in response to excitatory inputs from the MC neuron and accelerates the action potential upstroke.

Our second finding concerns the native behavior of the EXP-2 potassium channel. When expressed in a heterologous system, *Xenopus* oocytes, EXP-2 behaves as an inward rectifier: it conducts very little current at potentials more positive than the equilibrium potential for potassium. This is due to its peculiar kinetics: the inactivation is much faster than the recovery from inactivation at positive potentials. Surprisingly, we show that in its native environment, in the pharynx, EXP-2 conducts large outward currents at positive potentials. Thus, the property of ultrafast inactivation in response to hyperpolarization is not observed in the native system. EXP-2 currents are effectively triggered by the hyperpolarization threshold, an unusual mechanism among ionic channels.

Materials and methods

Worm culture and strains

Worms were grown at 20°C on NGMSR plates seeded with *E. coli,* strain HB101. NGMSR is nematode growth medium (NGM; Sulston and Hodgkin, 1988) containing nystatin and streptomycin to prevent contamination (Davis et al., 1995). The wild-type *Caenorhabditis elegans* (Maupas, 1900) strain was Bristol (N2); mutant strains were: DA1651 *cca-1(ad1650) X* (Steger et al., 2005), MT1212 *egl-19(n582) IV* (Trent et al., 1983), DA1426 *exp-2(sa26 ad1426) V* (Davis et al., 1999) and DA1694 *egl-19(n582) IV; cca-1(ad1650) X*.

Recording and dissection chambers

For dissection and voltage clamp recordings, disposable chambers were made. A square piece of Parafilm with a 10 mm circle embossed with a Sharpie pen cap was placed on a clean 50 mm×30 mm coverslip (Fisher Scientific, Pittsburgh, PA, USA). It was covered with another coverslip, moistened by breathing on it to prevent sticking. This assembly was placed on a dry heating block at 70–90°C, thumb pressed for 3 s, and air-cooled. The upper slide was pried away with a razor blade and removed; the Parafilm stuck firmly to the bottom slide. Chambers were stored like this to keep the glass clean. The Parafilm circle was excised immediately before use, leaving a circle of clean glass surrounded by Parafilm. The chamber held up to 150 µl of solution.

Dissection procedure

Early gravid adult animals (2–2.5 days old) were used for experiments. They were transferred to a 100 µl drop of low calcium Dent's solution (see Solutions and Chemicals for all solutions) on a cooled dissection chamber. (A flat tissue culture flask filled with ice-cold water was used for cooling.) Under a dissection microscope, worms' heads were cut off with a hand-held 25-gauge syringe needle (Fig. 1B). The corpses were removed with 50 µl of buffer, then 50 µl of digestion mix 1 was added. The slide was placed on an Axiovert 35 inverted microscope (Zeiss, Germany). 10–15 pharynxes were processed in each batch.

Under 400× magnification, the cuticle covering the anterior half of the pharynx was removed using two glass pipettes (Fig. 1C). These dissection pipettes were made of 1.2/0.68 mm borosilicate glass (A-M systems, Carlsborg, WA, USA) by breaking micropipettes pulled on a P-2000 needle puller (Sutter Instruments, Novato, CA, USA), followed by heat polishing. The larger pipette was heat polished to 32–36 µm, the smaller one to 6–7 µm opening size. Pipettes were mounted in holders on UMM-3FC mechanical manipulators (You Ltd., Japan), aligned on one axis and positioned at an angle as small as possible to the microscope stage, to allow insertion of the smaller pipette into the larger one. To control suction, syringes were connected to pipettes.

While the pharynxes were digesting in mix 1, body wall removal (skinning) was performed as shown in Fig. 1C. The terminal bulb of the pharynx was sucked into the larger pipette. Then, the smaller pipette was attached to the front end of the pharynx and strong suction was applied to the small pipette by locking the piston of the 30 ml syringe as far out as it would go. The small pipette was then advanced into the big one, inverting the cuticle and the body wall covering the pharynx. At this point, the pressure in the small pipette was switched to atmospheric. By moving the small pipette back and fourth, the cuticle was torn off the pharynx; in cases when the inverted cuticle stayed attached we cut it off later with a hand-held 25-gauge syringe needle. Finally the pharynx was expelled from the big pipette. Cuticles and dead pharynxes were removed in 50 µl of solution, and 50 µl of digestion mix 2 was added. After 15–20 min digestion at room temperature, pharynxes were transferred with a pipette to a 100 µl drop of Dent's solution on a clean recording chamber.

Using the same small pipette that was used for skinning, pharynxes were positioned in the center of the chamber and attached to the glass by gently pressing them with the pipette. Dissection pipettes were removed to allow patch pipette access. After 2–3 min perfusion with the Dent's solution, recordings were started. All recordings were done at room temperature (22–25°C).

Voltage clamp recording

An Axoclamp 2B amplifier (Axon Instruments, Union City, CA, USA) equipped with an HS-2A 0.1LU recording headstage was used in the cSEVC (continuous single electrode

voltage clamp) recording mode. The headstage was mounted on an MHW-4 (Narishige, Japan) one-axis water hydraulic manipulator, which was fixed on a UMM-3FC manipulator. The amplifier was interfaced with a Pentium 3 Windows NT computer *via* a PCI-6035E E-Series DAQ-200 board (National Instruments, Austin, TX, USA) and controlled by custom-designed software developed in the Labview 6 environment (National Instruments). Amplifier settings were as follows: gain 3 nA/mV, phase lag 0.07 ms, multiplier 100, output bandwidth 3 kHz. Sampling rate was 4 kHz. Patch pipettes were produced from 1/0.58 mm borosilicate capillaries (A-M systems) on a P-2000 puller and heat-polished; they had resistances of 5.5–7 MΩ when filled with intracellular solution. After break-in to the whole-cell configuration by suction or mild buzzing, series resistance R_{series} was 10–15 MΩ. Series resistance compensation ('BRIDGE' knob in the cSEVC mode) and capacitance compensation were used as stability allowed. Preparations with initial R_{series}>15 MΩ could not be clamped. The bath solution was perfused by gravity flow at approx. 0.1 ml min^{-1} during recordings. During pulse protocols, we used 5 ms voltage ramps in informative voltage steps, or 40 ms ramps for non-informative steps instead of instantaneous (square) voltage steps. This greatly increased the survival of the pharynxes and overall success rate; square pulses to above 0 mV usually killed pharynxes.

The holding potential was –80 mV. The linear current component (leak current) was measured using 20 mV hyperpolarizing test pulses (from –80 to –100 mV) and subtracted during recordings.

In addition to inward currents (Fig. 2), in some experiments, depolarizing pulses evoked an outward current similar to a delayed rectifier K_v current (data not shown). This outward current was highly variable, from non-existent to very noticeable. In these experiments we observed strong contractions in response to depolarizing pulses. We tend to distrust these experiments, because we believe that in these experiments intracellular Ca^{2+} was poorly buffered, causing non-physiological changes during recording. Such preparations were discarded. We only chose preparations in which the intracellular calcium concentration $[Ca^{2+}]_i$ was apparently well buffered, as judged by the complete absence or hardly noticeable muscle contraction in response to the depolarization. Buffering $[Ca^{2+}]_i$ could certainly block some currents, for example calcium-activated K channels. However, in *Ascaris lumbricoides* pharynx no delayed rectifier current was observed, even when no attempt to buffer $[Ca^{2+}]_i$ was made (Byerly and Masuda, 1979).

Data analysis

Data were analyzed using Microsoft Excel and Labview. To measure activation time constants, current segments from 0 nA to the peak amplitude were fit to the monoexponential with the Levenberg–Marquardt algorithm in Labview. Data are presented as mean ± standard deviation (S.D.). In all figures voltage commands and currents are time-locked.

Sharp electrode voltage recordings

Sharp electrode voltage recordings were performed as described by Steger et al. (2005). To determine the slope of the action potential plateau phase, 30 action potentials from five pharynxes (six from each) were analyzed. For each action potential, the coordinates of the start and the end of the plateau phase were manually determined using Igor Pro software (Wavemetrics, Lake Oswego, OR, USA). The slope of these segments was averaged to obtain the average plateau phase slope.

Solutions and chemicals

Digestion mix 1 was prepared by mixing collagenases F and H (Sigma, cat. nos. C-7926 and C-8051) to adjust collagenase activity to 20 U ml l^{-1} and protease activity to 45 U ml l^{-1} in low calcium Dent's solution [same as Dent's solution (see below) except the Ca^{2+} concentration was 10^{-5} mmol l^{-1}]. Mix 2 contained (in U ml l^{-1}; all from Sigma): 20 collagenase, 600 protease (adjusted by mixing collagenases F and H), 13 protease X (cat. no. P-1512), 1300 trypsin (T-0303), 1 chitinase (C-6137) in low calcium Dent's solution. Modified Dent's solution (Dent and Avery, 1993) was used as an extracellular solution (in mmol l^{-1}): 140 NaCl, 6 KCl, 1 $MgCl_2$, 3 $CaCl_2$, 10 Na-Hepes, pH 7.3, osmolarity adjusted to 345 mOsm kg l^{-1} with xylitol. Intracellular solution contained (in mmol l^{-1}): 130 potassium gluconate, 10 NaCl, 5 K-EGTA, 0.5 $CaCl_2$, 1 $MgCl_2$, 10 K-Hepes, pH 7.3, osmolarity adjusted to 325 mOsm kg l^{-1} with xylitol. Nifedipine was from Sigma.

Pharynx capacitance calculation

The physical dimensions of the pharynx of an adult worm were taken from table 1 in Avery and Shtonda (2003). The total length of the pharynx is 144.7 μm. The perimeter of the interior lumen is 25 μm in the corpus and 20 μm in the isthmus and in the terminal bulb; the lengths of the corpus, isthmus and terminal bulb are 76.6, 35.8 and 32.3 μm. Therefore, the area of the internal lumen is 76.6×25+35.8×20+32.3×20= 3277 μm^2. (We assumed the lumen section in the isthmus and terminal bulb to be the same.) Using a pharynx micrograph, we found the outer radius of the pharynx at 100 points along its length (r_1–r_{100}). The area of the outer surface is a sum $\Sigma\{\pi(r_i+r_{i+1})\sqrt{[(r_i-r_{i+1})^2+L^2]}\}$=8939 μm^2 (from i=1 to i=99), where L is a step along the x axis (1.447 μm).

Thus, the total surface membrane area is 12216 μm^2. In various studies, the specific membrane capacitance was measured in the range 0.7–1.3 μF cm^{-2} (Curtis and Cole, 1938; Gentet et al., 2000). Assuming the specific membrane capacitance of 1 μF cm^{-2} (0.01 pF μm^{-2}), the surface capacitance is 122 pF. Next, we estimated the contribution of some internal membranes to the total capacitance. In the corpus and isthmus, there is an invagination in each muscle cell. Assuming that the depth of these invaginations is equal to the radius of the pharynx (figs 5 and 6 in Albertson and Thomson, 1976), the total area of invaginations is $6\Sigma[(r_i+r_{i+1})L/2]$= 5226 μm^2; they would contribute 52 pF of capacitance.

Three marginal cells run the length of the pharynx; and each

marginal cell has two lateral membranes that face pharyngeal muscle cells. It is not known whether marginal cells contract, but most likely they are charged because they appear to receive neuronal input (Albertson and Thomson, 1976), and gap junctions have been observed connecting them to the muscle cells (L.A., unpublished data). The total area M of lateral muscle cell and marginal cell membranes is $12\Sigma[(M_i+M_{i+1})L/2]=7231\ \mu m^2$ where $M_i=0.7\ r_i$ in the isthmus and $0.6\ r_i$ in the corpus, as estimated from figs 5 and 6 in Albertson and Thomson (1976). These membranes would add 72 pF to the total capacitance.

Finally, we included membranes that connect different layers of muscle cells, as deduced from fig. 21 in Albertson and Thomson (1976). These membranes would contribute at least 30 pF (their invaginations were not included).

Thus, the total membrane capacitance of the pharynx is 122+52+72+30=276 pF. We assumed capacitances of pharyngeal cells to be in parallel, so that they add up to produce the maximum possible total capacitance. If some capacitances are in series, they would reduce the total capacitance. However, some membranes that lie within the pharynx, such as those lining cavities in the terminal bulb where gland cells reside or those of the terminal bulb marginal cells, were not included in this calculation because of their convoluted shape, and some internal membranes that were included are not flat and contain invaginations. These simplifications could result in underestimation of the capacitance. Because of the uncertainties in membrane area and the lack of a direct measurement of the specific capacitance of pharyngeal muscle membrane, this is a very rough estimate, probably only reliable to within a factor of two.

Results

A whole-cell voltage clamp for the pharynx

The pharynx poses three main problems for voltage clamp experiments. First, the pharynx is not one electrically uniform cell; it is a structure of 60 cells, of which 20 are muscle cells connected by gap junctions. The second problem is a tough basement membrane covering the pharynx, which prevents formation of gigaseals. Finally, the pharynx has a low resistance and generates large currents in response to voltage pulses, which makes clamping the voltage difficult.

Functionally and anatomically, the pharynx can be divided into three major compartments: the corpus, the isthmus and the terminal bulb (listed from anterior to posterior; Fig. 1A). When a worm's head is cut off, the body wall muscles underlying the cuticle contract and the terminal bulb falls out, while the corpus remains covered (Fig. 1B). When we and others (Davis, 1999) attempted to voltage clamp the pharynx *via* the terminal bulb, the corpus apparently could not be clamped and fired action potentials in response to depolarizing voltage pulses. Empirically, we found that the pharynx could be clamped *via* the corpus if a patch electrode seals on the pm4 muscle cell (Fig. 1A, area of patching is shaded). To make the corpus accessible to a patch electrode, we devised a microdissection procedure. Using two glass pipettes, the cuticle covering the pharynx was inverted and torn off (Fig. 1C). Then, the pharyngeal basement membrane was digested with enzymes, and the pharynx was attached to the glass slide (Fig. 1D).

We do not fully understand why it is possible to voltage clamp the pharynx *via* one, but not the other compartment. It is probable that the corpus has lower resistance than the terminal bulb and is a more powerful current source, which is suggested by the fact that the relaxation transients of the terminal bulb, recorded by electropharyngeogram, are about six to tenfold smaller than those of corpus (Raizen and Avery, 1994). In this case, currents that leak into the terminal bulb from the corpus will be large compared to the currents measured in the terminal bulb, whereas currents that leak into the corpus from the terminal bulb will be small compared to the currents measured in the corpus. When we clamped pharynxes *via* the corpus, we did not see interference that looked like current injections from neighboring poorly clamped cells. Therefore, either the terminal bulb is clamped well from the corpus, so it cannot interfere, or, it is clamped

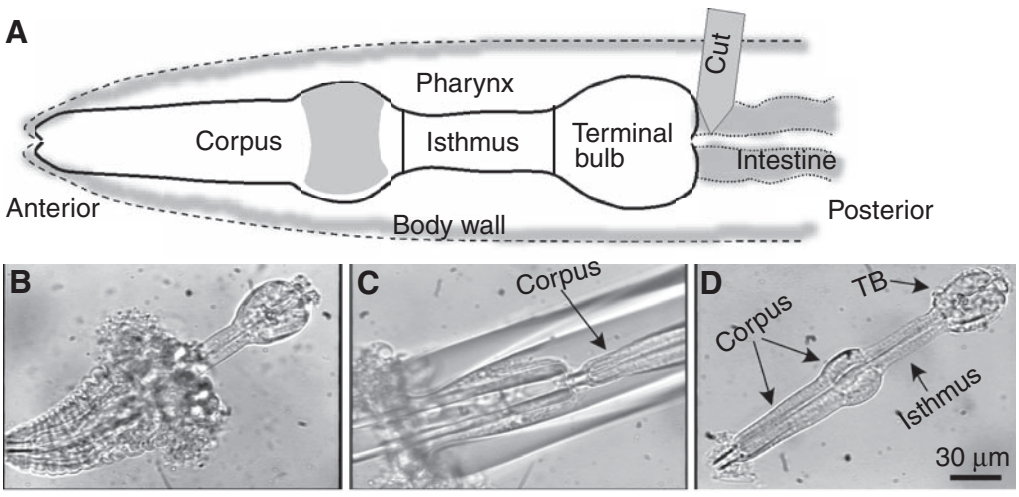

Fig. 1. The pharynx skinning procedure. (A) Schematic of the *C. elegans* pharynx as it is positioned in the worm's head. To dissect the pharynx, the head is cut off between the pharynx and the intestine. Three compartments of the pharynx are shown. Area of patch pipette attachment (shaded area of the corpus) roughly corresponds to the pm4 muscle cell of the pharynx. (B) Cut-off worm's head. (C) Body wall inversion using two pipettes. The smaller pipette (left) is pushed into the bigger one, inverting the body wall. (D) Skinned and digested pharynx, before patching. TB, terminal bulb.

poorly but it does not have the ability to interfere, because it is not as electrically active as corpus. We could not test how well the terminal bulb is clamped, because we could not measure its membrane potential with another electrode.

Mechanically, the pharynx is a very rigid structure – during contractions its inner lumen opens, while its outer shape does not change. Because the pharynx is attached to other tissues only at its very front and back ends, this mechanical rigidity is entirely conferred by the pharyngeal basement membrane. In order to be able to form gigaseals, we had to use rather harsh digestion with a mixture of collagenases, proteases and chitinase. It is certainly possible that as a result of this digestion, the physiology of the pharynx changes, and we cannot test this because we cannot record from undigested pharynxes. One of the reasons why we think these changes are not too dramatic is because digested pharynxes still contract spontaneously and fire trains of action potentials in response to current injection (data not shown).

Electrical parameters of the wild-type pharynx are as follows: input resistance 22.8±5.2 MΩ, capacitance 362.6±36.8 pF, equilibrium potential for the leakage current –53.6±4.1 mV (N=29). Current densities (normalized to the cell capacitance) are comparable to those in body wall muscle. For example, EGL-19 currents in the body wall have a peak density of 7 A/F (Jospin et al., 2002a). In the pharynx, the maximal density of the high voltage-activated current is about 12 A/F (see Fig. 3A, see text below). For CCA-1 and especially EXP-2 currents, peak densities are much higher; up to 50 A/F (up to 18 nA in current amplitude). Our results (see below) suggest that CCA-1 and EXP-2 currents function at the start and at the end of the action potential; thus, they must be large to rapidly charge the membrane capacitance. In comparison with EGL-19 currents recorded in the body wall muscle, which have peak amplitudes of 0.5 nA (Jospin et al., 2002a), pharyngeal currents are very large in amplitude.

As expected for a multicellular structure, good voltage clamp could not be achieved, so that voltage escape is evident at the inward current activation threshold (Fig. 2). However, because of the availability of mutants in *C. elegans*, we still could identify ion channels that conduct major currents. In theory, it is nearly impossible to voltage clamp a cell with a resistance of 20 MΩ and currents of 10–20 nA *via* a single patch electrode with a series resistance of 10 MΩ (Sherman-Gold, 1993). We found empirically that if the amplifier gain is kept low (see Materials and methods) we could maximize clamp stability, although the speed of the clamp was sacrificed. Another trick we employ is using 5 ms voltage ramps instead of square pulses. If square pulses are applied, capacitive currents of more than 50 nA are injected, followed by the pharynx breaking down.

In order to see whether or not we fully charge the pharynx in our voltage clamp, we compared its measured capacitance with a crude estimate based on geometry (see Materials and methods). The calculated capacitance, deduced from its membrane area, is approximately 276 pF. The calculated capacitance is smaller than the measured capacitance (363 pF), suggesting that the former is an underestimate that cannot be used as the only way to estimate the voltage clamp efficiency. But within the possible uncertainty of the estimate, this result is at least consistent with the hypothesis that most of the capacitance is charged.

The large CCA-1 and EXP-2 currents evidently function to rapidly charge membrane capacitance at the start and at the end of the action potential upstroke. Thus, the physiologically relevant pharyngeal capacitance can be estimated. In voltage recordings, the peak rate of the voltage change during upstroke reaches 20 V s^{-1} (Steger et al., 2005). The peak CCA-1 current amplitude is about 8 nA (Fig. 2A). Because for capacitive current $I=C(\mathrm{d}V/\mathrm{d}t)$, this active current can charge a capacitance of about 400 pF, which is close to the measured capacitance of 363 pF. Therefore, crude estimates of the pharyngeal capacitance, based either on its structure or on the size of active currents, are consistent with the experimentally measured capacitance. This suggests that most of the pharyngeal capacitance is charged in our voltage clamp experiments.

CCA-1 is a T-type calcium channel that mediates the low voltage-activated current in the pharynx

In response to step depolarizations from a holding potential of –80 mV, an inward current is activated (Fig. 2). In wild-type pharynxes, there is a low-voltage activated (LVA), quickly inactivating component in this inward current, which looks like a conventional T-type calcium channel current (N=29; Hille, 2001). CCA-1 is a calcium channel alpha subunit in *C. elegans* homologous to mammalian T-type calcium channel alpha 1 subunits (Steger et al., 2005). In worms *cca-1*::*GFP* fusion protein is expressed in a variety of tissues, including the pharyngeal muscle (Steger et al., 2005). Pharynxes of a *cca-1(ad1650)* null mutant did not exhibit the LVA current (N=19; Fig. 2A). In order to isolate the non-LVA component of the inward current in the wild type, we used a prepulse voltage protocol. A 300 ms prepulse to –40 mV activates and inactivates the LVA current, revealing a high voltage-activated (HVA), slowly inactivating component (Fig. 2B). The HVA current is the same in the wild type and in *cca-1*. Consistent with the pharmacology of calcium channels, both HVA and LVA currents are blocked by 2 mmol l^{-1} Ni^{2+} (Fig. 2C). In our system T- and L-type currents seemed to be equally sensitive to Ni^{2+} and we only saw an effect at rather high concentrations, starting with 0.5 mmol l^{-1}. Both T-type and HVA vertebrate channels are also sensitive to these concentrations of Ni^{2+} (Hille, 2001). Among vertebrate T-type alpha subunits, only α_{1H} is highly sensitive to block by low Ni^{2+} concentrations, with IC_{50}=13 μmol l^{-1} (Lee et al., 1999), so the Ni^{2+} sensitivity of the pharyngeal LVA current is consistent with most known T-type channels. The HVA but not the LVA current is partially blocked by the L-type calcium channel blocker nifedipine (Fig. 2D).

Current–voltage dependencies of LVA and HVA currents for wild type (N2) and *cca-1* are shown in Fig. 3. The LVA current activates starting from –40 mV, reaching a maximum at –30 mV. The HVA current starts to activate at about

–10 mV, reaching a maximum at about +20 mV. Finally, it is interesting to note that the pharyngeal muscle of *C. elegans*, unlike the body wall muscle (Richmond and Jorgensen, 1999), does not show a noticeable delayed rectification, except under special circumstances (see Materials and methods). This is also

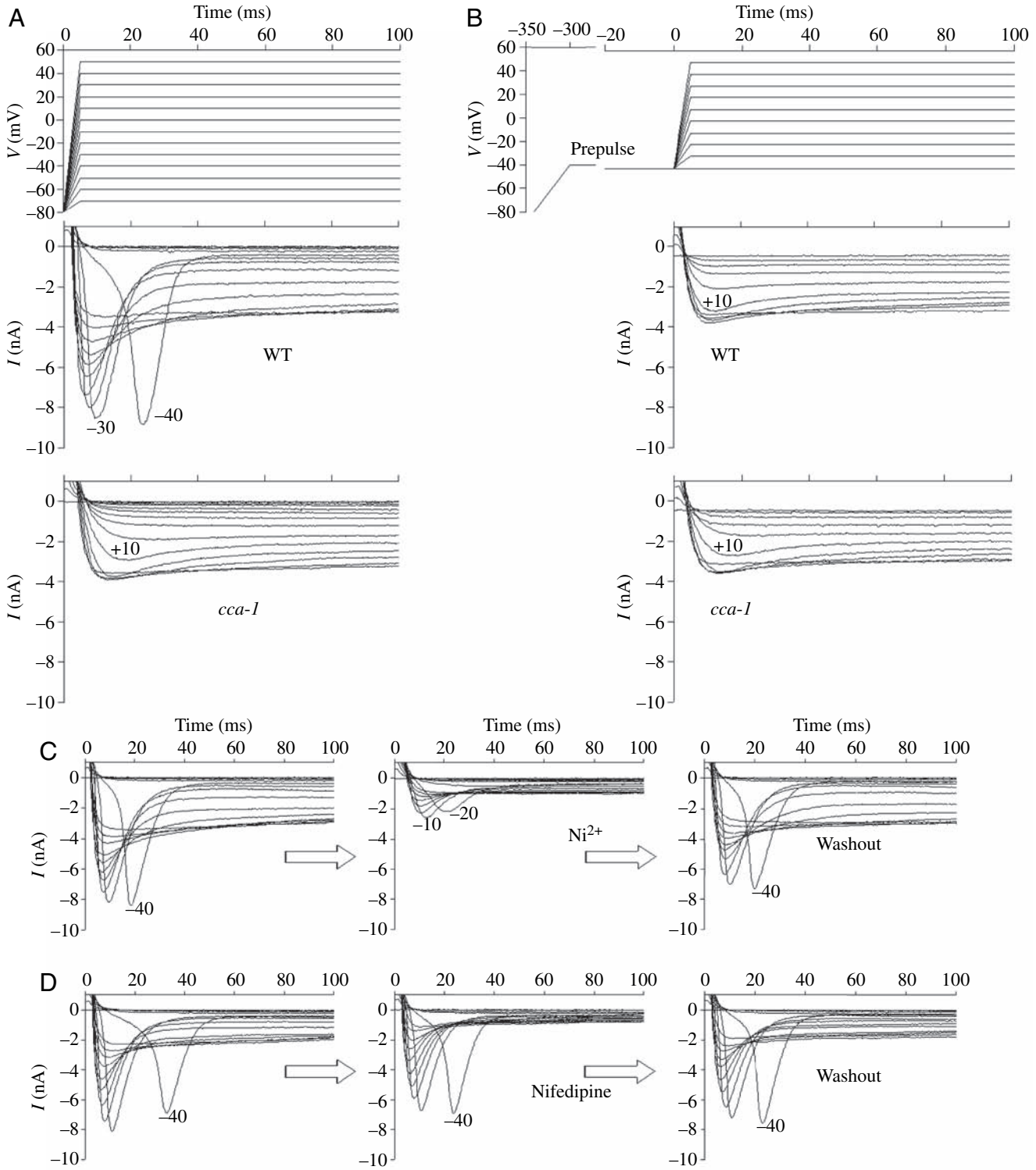

Fig. 2. Depolarization-activated inward currents in the pharynx. (A) Total inward currents in the wild type (WT) and in the *cca-1* mutant. (B) High voltage-activated (HVA) currents in the WT and in *cca-1*. In these experiments the low voltage-activated (LVA) current was inactivated with a 300 ms prepulse to –40 mV. (C) Ni^{2+} (2 mmol l^{-1}) blocks both the LVA and the HVA currents. (D) Nifedipine (10 µmol l^{-1}) blocks the HVA, but not the LVA current. Recordings in C and D are from wild-type pharynxes, and the pulse protocol is the same as in A. Numbers next to current traces indicate peak depolarization of the voltage pulse.

true for another nematode, *Ascaris lumbricoides* (Byerly and Masuda, 1979).

Our results suggest that CCA-1 is a true worm T-type calcium channel ortholog with typical T-type kinetics, voltage dependency and pharmacology. We have not, however, determined whether CCA-1 is selective for Ca^{2+}, because of the sensitivity of the pharynx preparation to low sodium or EGTA in the bath solution.

EGL-19 mediates the high-voltage activated current in the pharynx

By their high voltage activation and slow inactivation, HVA currents recorded from the pharynx look very similar to L-type calcium channel currents (Hille, 2001). They are also similar to L-type currents recorded in *C. elegans* body wall muscle (Jospin et al., 2002a). Nifedipine, a dihydropyridine L-type calcium channel antagonist, blocks the HVA current (Fig. 2D). (In contrast to the body wall L-type current, which is blocked by 1 μmol l^{-1} nifedipine, we only saw an effect starting from 5 μmol l^{-1}.) Other channels may also be affected by these rather high nifedipine concentrations, but in our system it only affected the HVA, not the LVA current.

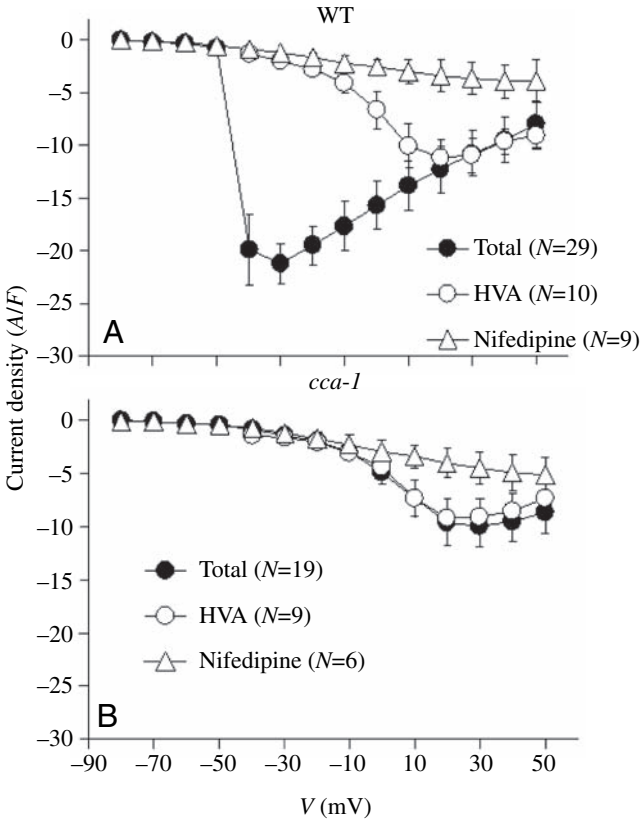

Fig. 3. Current–voltage (*I–V*) relationships for inward currents in the wild-type and *cca-1* pharynxes. (A) Wild type. (B) *cca-1*. Voltage protocols for the total current and current in the presence of 10 μmol l^{-1} nifedipine were the same as in Fig. 2A: depolarizing pulses were applied in 10 mV increments starting from the holding potential of –80 mV. HVA currents were measured with the same voltage protocol as in Fig. 2B: LVA current was inactivated with the prepulse to –40 mV. For nifedipine experiments, averaged current values at 50–60 ms of the pulse were used (after the LVA current has inactivated); otherwise, peak amplitudes were used for *I–V* curves.

EGL-19, a *C. elegans* L-type calcium channel alpha subunit, has previously been implicated in pharyngeal physiology: hypomorphic mutations in *egl-19* cause feeble pumping, whereas gain-of-function mutations cause extended terminal bulb contractions. In hypomorphic mutants such as *egl-19(n582)* (Trent et al., 1983) the slope of the rising phase of the action potential is smaller than in the wild type (Lee et al., 1997). *n582* is an arginine to histidine substitution in the S4 voltage sensor segment of the channel, but it is not a null mutation; unfortunately, *egl-19* null mutants are embryonic lethal (Lee et al., 1997). We found that in the *egl-19(n582)* hypomorphic mutant the activation of the HVA current is clearly delayed (Fig. 4A,B). This is observed both in the *cca-1* background where LVA currents are conveniently absent (Fig. 4A) and in the wild type with a prepulse voltage protocol (Fig. 4B). Activation-time constants in *n582* are significantly larger than in the wild type at pulses to 30, 40 and 50 mV (Fig. 4D). Consistent with the study of the same mutation in the body wall muscle (Jospin et al., 2002a), the current–voltage dependence in *n582* is shifted by about 10 mV to the right (Fig. 4C); however, in contrast to the body wall, the peak current amplitude is not decreased compared to the wild type. This could be explained by a compensatory increase of mutant EGL-19 expression in the pharynx. For example (Steger et al., 2005) have shown that compensatory changes in pharyngeal currents occur if MC neurotransmission is lost, suggesting that pharyngeal excitability is tightly feedback regulated. Alternatively, the effect of *n582* on the pharyngeal EGL-19 could be different because of different non-alpha subunits.

Jospin et al. (2002a) recorded much lower time constants – as small as 0.5 ms for the wild type *vs* 2 ms in our recordings. We think that this difference is due to the slow speed of our voltage clamp, which does not allow faster rise times to be measured. Our kinetic measurements are therefore specific to our system; but we can detect differences between the wild-type and mutant L-type channel within this system. The effect of the *n582* mutation on the HVA current rise time is also consistent with its effect on the speed of the action potential upstroke described by Lee et al. (1997). Our results suggest that EGL-19 conducts a major component of the HVA current in the pharynx. Based on its voltage dependence and kinetics, the most probable role of EGL-19 is in maintaining the action potential plateau phase.

A certain component of the depolarization-activated current is not blocked by either Ni^{2+} or nifedipine. This component shows almost no inactivation (Fig. 2C,D) and has very shallow voltage dependence (Fig. 3A,B). It is unlikely to be a residual L-type current because its voltage dependence is very shallow and totally different. It is also unlikely to be a T-type current because it is unchanged in *cca-1*. Most probably, this is a weakly voltage-dependent, leakage-like conductance.

EXP-2 generates outward current in response to hyperpolarization

Byerly and Masuda (1979) described a negative spike potassium current in the pharyngeal (also called esophagus) muscle of the parasitic nematode *Ascaris lumbricoides.* This current activates in response to step hyperpolarization of a depolarized muscle. In studies by Wayne Davis and colleagues (Davis, 1999; Davis et al., 1999), the potassium channel EXP-2 has been proposed to be the negative spike channel in the pharyngeal muscle of *C. elegans*. According to the amino acid sequence, EXP-2 is a potassium channel of the kV family, and a single member of its own subfamily (Fleischhauer et al., 2000). By analyzing mutants, Davis (1999) showed that EXP-2 regulates action potential duration in the *C. elegans* pharynx by initiating rapid repolarization at the end of the plateau phase of an action potential. Normally, action potentials last for about

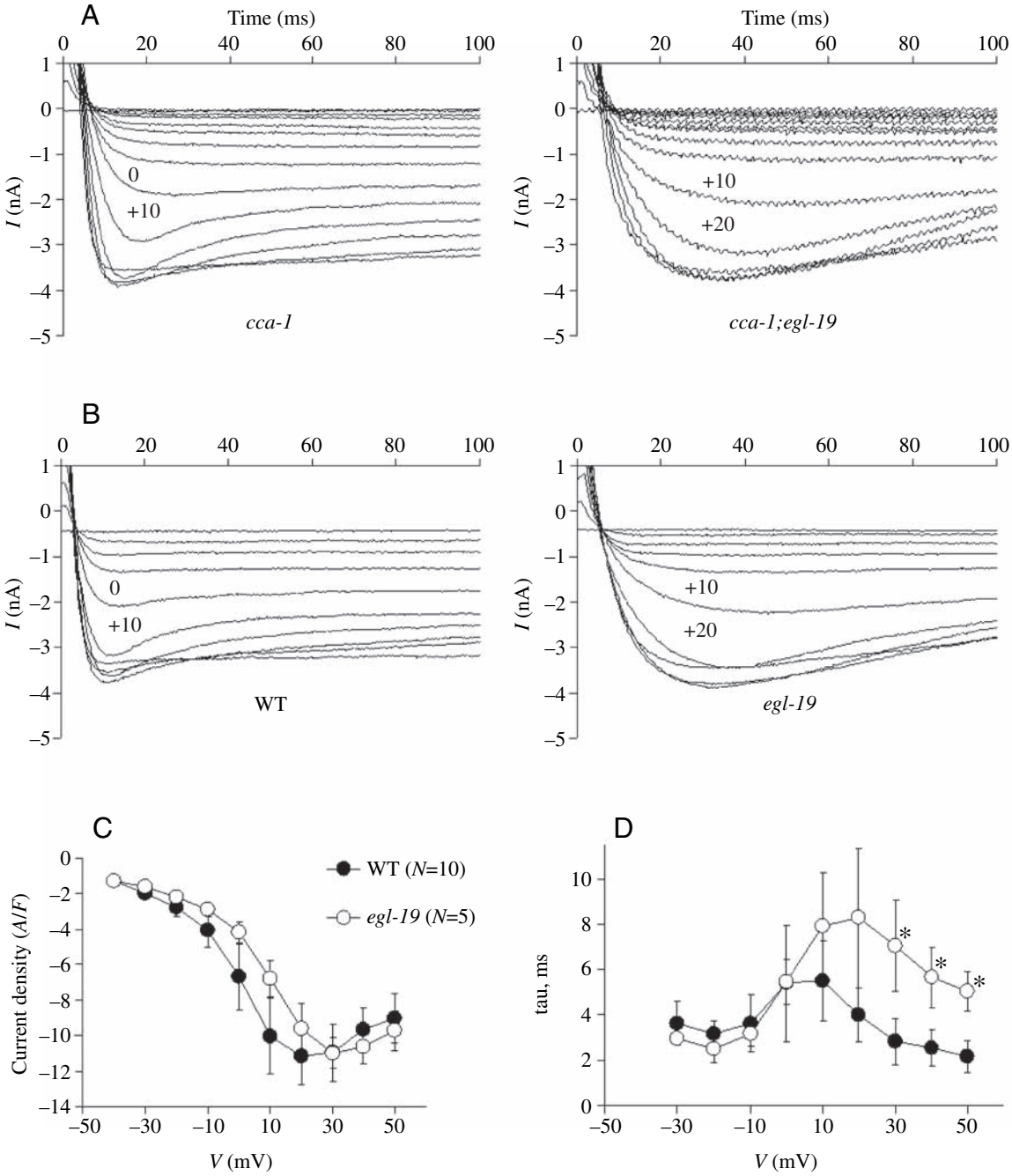

Fig. 4. The EGL-19 L-type calcium channel conducts the HVA current in the pharynx. (A) Total currents in *cca-1* and *cca-1; egl-19.* 100 ms depolarizing pulses were applied in 10 mV increments from the holding potential of –80 mV (same protocol as in Fig. 2A). (B) HVA currents in wild type and *egl-19*. The LVA current was inactivated with a 300 ms prepulse to –40 mV (same protocol as in Fig. 2B). (C) Current–voltage dependencies of HVA currents in WT and *egl-19* (peak amplitudes; prepulse protocol). (D) Activation time constants of HVA currents in WT and *egl-19*; *significantly different by *t*-test, $P<0.01$.

100–250 ms, and in *exp-2* null mutants they are extended up to 6 s. In contrast, in *exp-2* gain-of-function mutants action potentials are shortened to about 50 ms.

When it is expressed in *Xenopus laevis* oocytes, EXP-2 behaves as an inward rectifier with properties similar to mammalian HERG (Fleischhauer et al., 2000). Kinetic measurements on EXP-2 expressed in *Xenopus laevis* oocytes have shown that the inward rectification of this channel results from its ultrafast inactivation (Fleischhauer et al., 2000), similarly to mammalian HERG (Spector et al., 1996). While the channel activation and deactivation are relatively slow in a wide voltage range (apparent time constants are of the order of 100 ms; fig. 5 in Fleischhauer et al., 2000), the inactivation rate is extremely fast: time constants are of the order of 1 ms. Because inactivation is faster than activation, EXP-2 does not conduct in response to depolarization (fig. 2 in Fleischhauer et al., 2000). Depolarization-activated outward currents in oocytes are small and very transient, lasting at most for 10 ms (fig. 4 in Fleischhauer et al., 2000).

More significantly, EXP-2 expressed in oocytes fails to conduct upon hyperpolarization to voltages more positive than the equilibrium potential for K^+, since at those potentials it remains inactivated. Yet in the pharynx, it must generate an outward, hyperpolarizing current, causing a negative spike, when the membrane potential is about 0 mV, much more positive than E_{K+}. This function of EXP-2 is predicted by studies in both *Ascaris* (Byerly and Masuda, 1979; del Castillo and Morales, 1967) and *C. elegans* (Davis, 1999; Davis et al., 1999). Thus Fleischhauer et al. (2000) concluded that the properties of oocyte-expressed EXP-2 are not well suited for its suggested role. We find, however, that in the pharynx, its native environment, EXP-2 is not an inward rectifier. It conducts large outward currents at potentials far more positive than the E_{K+} (Fig. 5A). These currents are absent in the *exp-2(ad1426)* null mutant. (Note that an inward current in *exp-2(ad1426)* is most likely an EGL-19 tail current.) Starting from +20 mV and going more negative, the current–voltage dependence of EXP-2 is almost linear, with no signs of inward rectification (Fig. 5B). This is similar to the voltage dependence of the negative spike current in *Ascaris* pharynx, except that in *Ascaris* this current starts from the hyperpolarization to –15 mV (Byerly and Masuda, 1979). The reversal potential of EXP-2 current is close to the predicted E_{K+} under these conditions (–82 mV). As expected, currents rise faster at more negative potentials, indicating strong voltage dependence of recovery from inactivation.

Our results suggest that EXP-2 is a channel with unusual properties, which is effectively opened by hyperpolarization beyond the deinactivation threshold.

Action potential duration is controlled by the slope of the plateau phase

During the action potential plateau phase, the membrane slowly repolarizes (Davis et al., 1995), presumably because of slow EGL-19 inactivation. During this time, EXP-2 falls into a ‘primed’ activated, but inactivated state. At some point, rapid

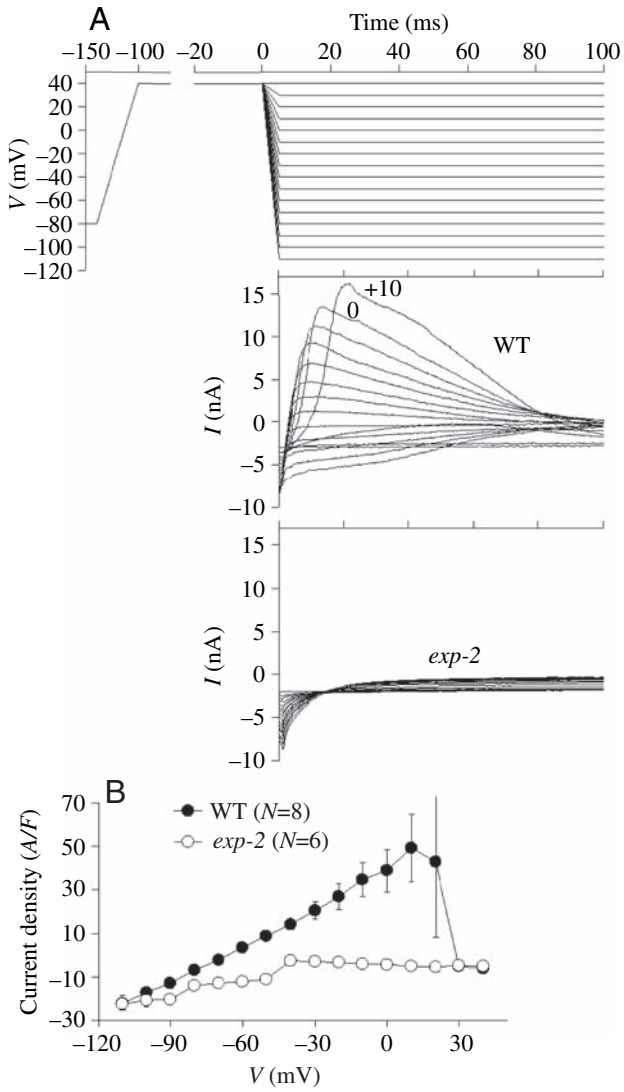

Fig. 5. EXP-2 conducts hyperpolarization-activated outward current. (A) Sample recordings from the WT and *exp-2*. (B) Current–voltage (*I*–*V*) relationships (peak amplitudes).

recovery from inactivation occurs and an outward current spike arises, causing rapid repolarization. We were interested in how the shape of an action potential, particularly of a plateau phase, affects the timing of the EXP-2 spike. Using voltage recordings, we determined that in the wild type, the peak membrane potential during upstroke was 33±4 mV and the slope of the plateau phase was –0.22±0.06 V s^{-1} (30 action potentials from five pharynxes; see Materials and methods). Then, we voltage clamped pharynxes under two pulse protocols. To test the ramp effect, we depolarized pharynxes from the holding potential of –80 mV to 33 mV and then applied varying negative voltage ramps (Fig. 6A). To test the effect of the action potential amplitude, we depolarized pharynxes to different potentials and then applied the same ramp of –0.22 V s^{-1} (Fig. 6B). Under the varying ramp protocol, current transients appear starting from –30 mV at fast ramps and then at 0 mV (Fig. 6B). These are EXP-2 currents, since they are absent in the *exp-2* null mutant (*N*=2, data not

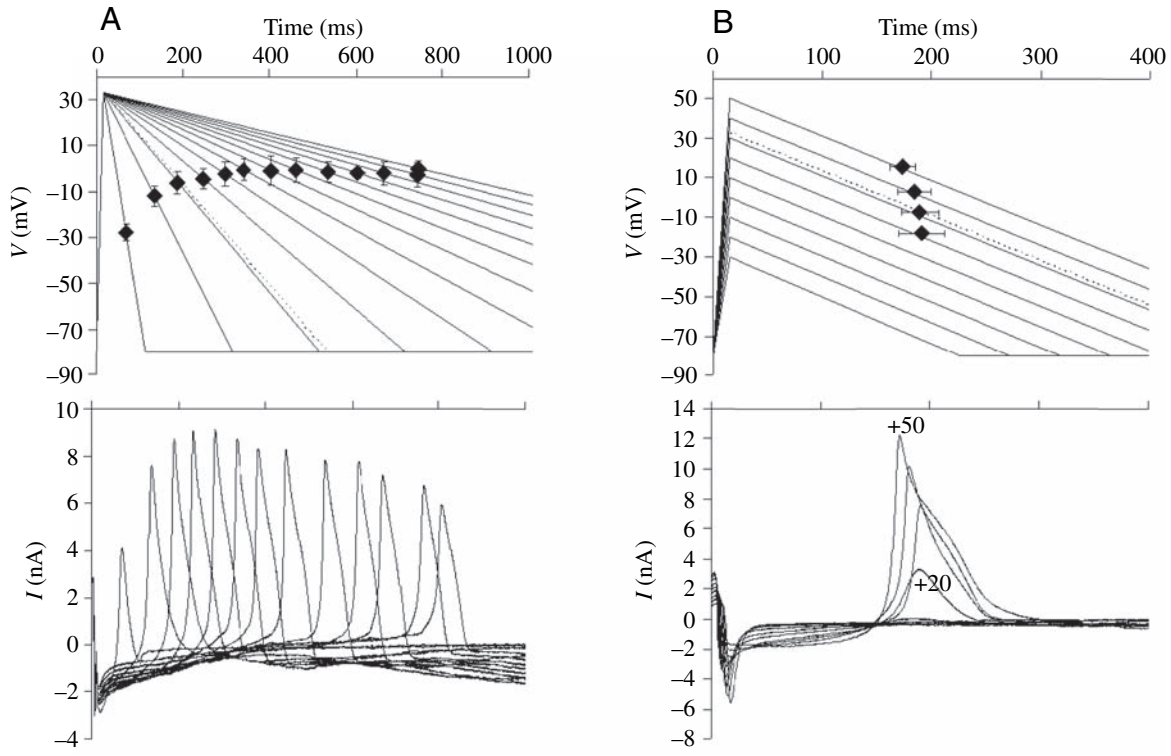

Fig. 6. The slope of the plateau phase determines the onset of the EXP-2 current. (Top) voltage commands; (bottom) corresponding currents from one pharynx. (A) Outward currents in response to varying voltage ramps starting from the same depolarization to +33 mV. (B) Outward currents in response to varying peak depolarizations followed by the same negative ramp of –0.22 V s^{-1}. On command voltage traces, average timings of EXP-2 current transients are indicated by black diamonds (*N*=4 pharynxes), and dotted lines show parameters of the wild-type pharynx, as determined by voltage recordings. For clarity, standard deviations for the voltage only are shown in A, and for the timing only are shown in B. All recordings are from wild type.

shown). Under the varying depolarization/constant ramp protocol, currents start at peak depolarizations to +20 mV, but, interestingly, with increasing depolarization, the potential at which the EXP-2 current transient develops increases by the same increment in such a manner that the time when the current develops is almost unchanged (about 200 ms). These results suggest that EXP-2 is tuned to generate a current spike once the membrane potential has dropped by a certain value, approximately 30 mV, from the peak depolarization. Thus, the latency of the EXP-2 current and the timing of the repolarization onset is effectively regulated by the ramp of the action potential plateau phase; the action potential amplitude has very little effect once some minimum depolarization has been reached (about +20 mV in our recordings). How could such regulation work? Most probably, it is explained by the voltage dependence of EXP-2 activation: at more positive voltages, the activation occurs faster, so channels more quickly become available for the recovery from inactivation (Fleischhauer et al., 2000). Because EXP-2 activation is relatively slow (Fleischhauer et al., 2000), it is limiting in determining the EXP-2 current timing under these conditions. Activation also limits the number of available channels, as seen from larger EXP-2 current amplitudes following larger peak depolarizations. As seen in Fig. 6A, the voltage at which EXP-2 current develops is lower with very fast ramps, probably because under these conditions activation is again limiting – even though EXP-2 deinactivates rapidly, there is no current until enough activation is achieved. When activation reaches saturation, the potential at which current develops does not change, it stays at about 0 mV, and its onset is completely determined by the recovery from inactivation voltage dependence. It is indeed remarkable how nicely EXP-2 kinetic properties are tuned to control the action potential duration.

Discussion

A model for the pharyngeal action potential

Here, we identify three ionic currents in the *C. elegans* pharynx. Based on properties of these currents and previous knowledge, we propose a qualitative model for the pharyngeal action potential (Fig. 7). Motor neuron MC excites the pharynx *via* the EAT-2/EAT-18 nicotinic acetylcholine receptor. Neurotransmission from MC depolarizes the membrane to about –30 mV, which triggers CCA-1 activation. (This is best shown in intracellular recordings from the *cca-1* mutant, where the MC transients reach about –30 mV and then plateau; see fig. 4D in Steger et al., 2005.) CCA-1 gives rise to a large, quickly inactivating inward current, which drives rapid membrane depolarization. Starting from –10 mV, EGL-19 is activated. Ca^{2+} influx *via* EGL-19 activates muscle contraction

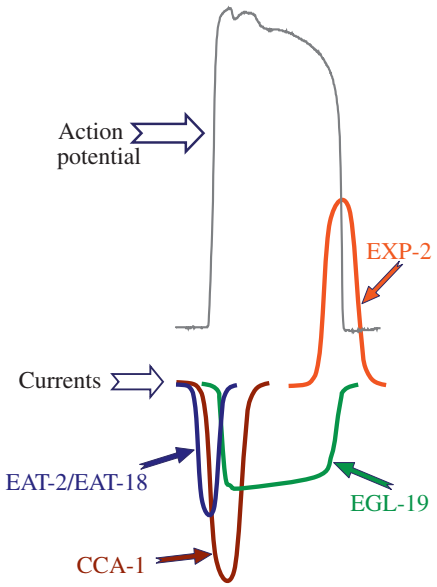

Fig. 7. Model of the pharyngeal action potential. Currents are not drawn to scale. Currents resulting from M3 neurotransmission are omitted for clarity.

and maintains depolarization during the plateau phase. As EGL-19 inactivates slowly, presumably in a Ca^{2+}-dependent way, the membrane repolarizes; finally it reaches the threshold for the EXP-2 recovery from inactivation. Inhibitory neurotransmission from the M3 neuron *via* AVR-15 channel speeds up the repolarization. When this threshold is reached, EXP-2 generates a large outward current, causing rapid membrane repolarization and termination of the action potential.

Our model does not provide a quantitative description of the voltage change during the action potential. We were unable to achieve the high-compliance voltage clamp required for kinetic measurements. We can, however, identify pharyngeal ion channels by the effect of mutations. CCA-1 and EXP-2 currents were identified by their complete absence in the respective null mutants, which was very obvious despite the imperfect clamp. The effect of an EGL-19 hypomorphic mutation is less striking but significant and consistent with previous reports. Furthermore, this model makes predictions about the effects of mutations on pharyngeal behavior, some verified by previous work (Davis et al., 1999; Lee et al., 1997), and some confirmed in the accompanying paper (Steger et al., 2005).

CCA-1 functions in the action potential rising phase

We here report one *in vivo* function of the *C. elegans* T-type calcium channel ortholog CCA-1. We show that CCA-1 generates an inward current in response to the depolarization. In the accompanying paper (Steger et al., 2005), we present evidence that CCA-1 aids in neurotransmission from MC to the pharyngeal muscle, and is necessary for the MC EPSP (excitatory post-synaptic potential) to rapidly and reliably trigger a muscle action potential. This is similar to the role of the T-type calcium channel in other systems. In the mammalian sino-atrial node, T-type current triggers an action potential after the hyperpolarization-activated inward current (I_f) brings the membrane potential to its activation threshold of about –50 mV (DiFrancesco, 1993; Hagiwara et al., 1988). Starting from –20 mV, L-type currents are activated. Similarly to the heart pacemaking tissue, T-type and L-type calcium channels function in concert in the pharyngeal muscle.

Interestingly, the T-type current has not been recorded in *Ascaris* (fig. 3 in Byerly and Masuda, 1979). But of course T-type calcium channels were not known at that time, so the authors of that study did not attempt to look for them and clamped cells at the holding potential of –37 mV, at which the T-type calcium channel is probably inactivated. So the depolarization-activated inward current in *Ascaris* pharynx looks much like the *cca-1* mutant response (compare Fig. 2 in our paper and fig. 3 in Byerly and Masuda, 1979).

EXP-2 displays unique properties in its native environment

In studies of the pharyngeal muscle of the parasitic nematode *Ascaris lumbricoides* it was noted that in addition to positive-going action potentials evoked by the depolarizing pulses, negative spike action potentials in the depolarized membrane can be evoked by small hyperpolarizing pulses (del Castillo et al., 1964; del Castillo and Morales, 1967). (The name ‘negative spike’ reflects the fact that these events are similar to the ‘positive spike’, conventional action potentials resulting from the Na^+ channel opening, but they are opposite in direction.) Byerly and Masuda (1979) determined that this current is carried by potassium and measured its voltage dependence and kinetics. Finally, work of Wayne Davis and collaborators (Davis, 1999; Davis et al., 1999) have shown that *C. elegans* EXP-2 potassium channel is likely to be the negative spike channel.

We show that EXP-2 conducts an outward current in response to hyperpolarization (Fig. 4). Our results suggest that properties of endogenous EXP-2 are similar, yet different from those observed when EXP-2 is expressed in *Xenopus* oocytes (Fleischhauer et al., 2000). Similarly to the oocyte-expressed channel, pharyngeal EXP-2 does not conduct upon depolarization, thus the property of ultrafast inactivation upon depolarization observed in oocytes is maintained in the native system. Also, the inactivation/deinactivation equilibrium is voltage-dependent in both oocytes and pharyngeal muscle, with positive membrane potential favoring inactivation. In oocytes the inactivation/deinactivation equilibrium is far towards inactivation even at 0 mV. But surprisingly, the deinactivation threshold appears to be much more positive in the pharynx, allowing for large outward currents lasting up to 80 ms at depolarized potentials as high as +20 mV (Fig. 5B). Thus, in contrast to the oocyte-expressed channel, pharyngeal EXP-2 does not inwardly rectify. EXP-2 current is triggered by membrane hyperpolarization to below the deinactivation threshold, which makes EXP-2 a channel with unusual properties, somewhat resembling those of the mammalian channel HERG (Spector et al., 1996) but otherwise unique.

These properties are ideally suited for the EXP-2 function in the pharyngeal muscle, which is to control the action potential duration by initiating rapid repolarization when the membrane potential is about 0 mV during the plateau phase.

That the EXP-2 properties in the heterologous system are different from the ones in the native environment is not very surprising. Other *C. elegans* ion channels require accessory subunits for their proper function, counterparts of which have not yet been found in vertebrates. For example, EAT-18 is required for the function of the pharyngeal nicotinic acetylcholine receptor (McKay et al., 2004), and SOL-1 protein is required for the function of the *C. elegans* GLR-1 glutamate receptor (Zheng et al., 2004). It is possible that other unknown subunits are needed for the wild-type function of EXP-2 as well.

Regulation of the pharyngeal muscle action potential duration

We show that the ramp of the action potential plateau phase determines the onset of the EXP-2 current and thereby regulates the action potential duration (Fig. 6A). It is the peculiar kinetic properties of EXP-2 that make this regulation possible. EXP-2 is tuned to generate a current spike once the membrane has hyperpolarized by approximately 30 mV from the peak depolarization.

The slope of the plateau phase might be regulated by the inactivation kinetics of the EGL-19 inward current. Mutations in a region of EGL-19 known to be important for channel inactivation cause dramatic elongation of pharyngeal action potentials (Lee et al., 1997), suggesting that EGL-19 inactivation is important in shaping the plateau phase. Extracellular Ca^{2+} concentration affects action potential duration: in lower extracellular Ca^{2+}, duration is extended (Dent and Avery, 1993). Barium at 1 mmol l^{-1} concentration causes extension of pharyngeal action potentials to over 1 s (Franks et al., 2002). Substitution of 6 mmol l^{-1} Ca^{2+} with 6 mmol l^{-1} Ba^{2+} slows the inactivation of the EGL-19 current in the body wall muscle (Jospin et al., 2002a). These observations are consistent with calcium-dependent inactivation mechanism of EGL-19. EGL-19 inactivation kinetics are critical for the shape of the plateau phase; thus, the amount of Ca^{2+} entry is likely to be the key factor in regulating the plateau phase slope, and, by affecting the timing of EXP-2 current, the action potential duration.

It is also possible that calcium-dependent potassium channels are involved in shaping the plateau phase, but this possibility was not tested because we had to buffer intracellular Ca^{2+} (see Materials and methods). In *Ascaris* esophagus, delayed rectifier potassium currents have not been observed, even though $[Ca^{2+}]_I$ was not buffered (Byerly and Masuda, 1979), which is in agreement with our results. Expression of the *C. elegans* calcium-dependent potassium channel gene *slo-1* (Wang et al., 2001) has not been detected in pharyngeal muscle, and *slo-1* mutations have no detectable effect on muscle function (Alan Chiang and L. A., unpublished results). The gene encoding a second calcium-activated potassium channel, *slo-2*, may be expressed in pharyngeal muscle (Yuan et al., 2000).

Another important factor that regulates action potential duration is the inhibitory motor neuron M3. The M3 neuron fires inhibitory postsynaptic potentials during the plateau phase of the action potential (Raizen and Avery, 1994), which presumably trigger the EXP-2 recovery from inactivation. But M3 does not play a major role in terminating the pharyngeal action potential: if this neuron is ablated, the pharyngeal contraction is only slightly extended (Avery, 1993b). Probably, it is the coordinated activity of the inward EGL-19 current and M3 that cause the EXP-2 recovery from inactivation, leading to the rapid membrane repolarization.

The unusual electrophysiology of the pharyngeal muscle is dictated by its function

If viewed as a single unit, the pharynx is likely the most active excitable structure in *C. elegans*. It is also a very large structure relative to the rest of the worm body, which is evidently dictated by the size of bacterial food and the physics of food intake. Hence there is a need for a powerful excitation mechanism.

C. elegans neurons are extremely small and have a very high phenomenological input resistance; most probably, they conduct excitation passively and do not need regenerative action potentials (Goodman et al., 1998). In the body wall, spontaneous activity is slow; and the action potential upstroke is more than 50 ms long (Jospin et al., 2002a). The pharynx is different: the membrane depolarization and repolarization during the action potential are both very rapid, less than 10 ms long. No close homolog of the voltage-gated sodium channel that mediates rapid events in vertebrates has been found in the *C. elegans* genome (Bargmann, 1998). Its role is played instead by CCA-1 in the pharyngeal muscle. Compared to currents recorded in other *C. elegans* excitable cells, CCA-1 current is huge – of the order of 10 nA, which evidently allows a very rapid charging of the membrane capacitance and drives a rapid action potential upstroke. Similarly to the role of CCA-1 in the upstroke, EXP-2 functions in the downstroke to rapidly terminate action potentials; EXP-2 currents reach 18 nA in amplitude. Presumably, large CCA-1 and EXP-2 currents allow fast, precisely timed muscle contractions. Indeed, pharyngeal muscle motions are much faster than those of body wall muscle, especially the relaxation. As del Castillo and Morales (1967) proposed, the "*efficiency of the esophagus as a pumping device*" depends on "*the sudden onset and relatively high speed of the relaxation process*".

Another possible reason why EXP-2 is needed is the apparent absence of substantial delayed rectifier-like potassium current in the pharynx. Most likely, the EXP-2 negative spike is a more precise and more advanced mechanism to control the end of the action potential than the delayed rectifier. The key difference between the negative spike repolarization mechanism and the delayed rectifier is that the latter is initiated by the depolarization during the action potential upstroke, so the onset of repolarization is inherently linked to the start of

the action potential. Negative spike current, in contrast, is activated by hyperpolarizations more negative than the deinactivation threshold, and is independent of the upstroke (except for very short durations, when channel activation becomes limiting, see Fig. 6). Therefore, the negative spike mechanism allows regulation of action potential duration over a very wide range (in *C. elegans*, from about 50 ms to more than 500 ms; B.S. and L.A., unpublished data), while keeping the repolarization rapid at any duration. Consistent with this hypothesis, EXP-2 current was not recorded in the body wall muscle (Jospin et al., 2002b; Richmond and Jorgensen, 1999), while the delayed rectifier current was not recorded in the pharynx (Fig. 2 in this paper and fig. 3 in Byerly and Masuda, 1979).

The pharynx possesses redundant mechanisms of excitation (Steger et al., 2005), which ensure its proper function and a wide range of adaptation. The rate of pharyngeal contractions is tightly regulated by various factors, such as developmental stage and mechanical stimuli (Keane and Avery, 2003), food availability (Avery and Horvitz, 1990) and food quality (Steger, 2003). Even extreme perturbations, such as laser ablation of the whole pharyngeal nervous system or getting rid of both MC and CCA-1 excitation mechanisms do not completely abolish pharyngeal function. In the latter case, the pharynx adapts by raising its resting membrane potential and by upregulating the leakage current (Steger et al., 2005).

In this study, we have treated the pharynx as a single functional unit. This is not totally appropriate: the timing and nature of electrical activity is different in different pharyngeal compartments, and precise control of these differences is critical for efficient food transport (Avery and Shtonda, 2003). For example, the relaxation of anterior isthmus has to slightly lag the corpus relaxation. Corpus and terminal bulb movements are rapid, whereas posterior isthmus contractions are slow and peristaltic and do not occur in synchrony with other compartments. Undoubtedly, differences in ion channel expression and regulation underlie some differences in the function of pharyngeal compartments. We predict, for example, that in the posterior isthmus, electrical activity is graded and CCA-1 and EXP-2 currents are absent; the isthmus may function similarly to body wall muscle. As electrophysiological techniques for the pharynx are improved, it will be possible to uncover how ion channels encode this amazingly precise regulation of electrical and contractile activity in different compartments of the pharynx.

We thank Kate Steger for helpful discussions and strains. We also thank Eric Jorgensen, Rolf Joho, Jim Waddle and the Terrance Snutch laboratory for commenting on the manuscript. This research was supported by National Institutes of Health research grant HL46154 (L.A.).

References

Albertson, D. G. and Thomson, J. N. (1976). The pharynx of *Caenorhabditis elegans*. *Phil. Trans. R. Soc. Lond. B* **275**, 299-325.

Avery, L. (1993a). The genetics of feeding in *Caenorhabditis elegans*. *Genetics* **133**, 897-917.

Avery, L. (1993b). Motor neuron M3 controls pharyngeal muscle relaxation timing in *Caenorhabditis elegans*. *J. Exp. Zool.* **175**, 283-297.

Avery, L. and Horvitz, H. R. (1989). Pharyngeal pumping continues after laser killing of the pharyngeal nervous system of *C. elegans*. *Neuron.* **3**, 473-485.

Avery, L. and Horvitz, H. R. (1990). Effects of starvation and neuroactive drugs on feeding in *Caenorhabditis elegans*. *J. Exp. Zool.* **253**, 263-270.

Avery, L. and Shtonda, B. B. (2003). Food transport in the *C. elegans* pharynx. *J. Exp. Biol.* **206**, 2441-2457.

Bargmann, C. I. (1998). Neurobiology of the *Caenorhabditis elegans* genome. *Science* **282**, 2028-2033.

Byerly, L. and Masuda, M. O. (1979). Voltage-clamp analysis of the potassium current that produces a negative-going action potential in *Ascaris* muscle. *J. Physiol.* **288**, 263-284.

Curtis, H. J. and Cole, K. S. (1938). Transverse electric impedance of the squid giant axon. *J. Gen. Physiol.* **21**, 757-765.

Davis, M. W. (1995). Intracellular recording from pharyngeal muscles. *Worm Breeder's Gazette* **13**, 34.

Davis, M. W. (1999). Regulation of the relaxation phase of the C. elegans pharyngeal muscle action potential. PhD dissertation, The University of Texas Southwestern Medical Center at Dallas.

Davis, M. W., Fleischhauer, R., Dent, J. A., Joho, R. H. and Avery, L. (1999). A mutation in the *C. elegans* EXP-2 potassium channel that alters feeding behavior. *Science* **286**, 2501-2504.

Davis, M. W., Somerville, D., Lee, R. Y., Lockery, S., Avery, L. and Fambrough, D. M. (1995). Mutations in the *Caenorhabditis elegans* Na,K-ATPase alpha-subunit gene, eat-6, disrupt excitable cell function. *J. Neurosci.* **15**, 8408-8418.

del Castillo, J., de Mello, W. C. and Morales, T. (1964). Hyperpolarizing action potentials recorded from the esophagus of the Ascaris lumbricoides. *Nature* **203**, 530-531.

del Castillo, J. and Morales, T. (1967). The electrical and mechanical activity of the esophageal cell of Ascaris lumbricoides. *J. Gen. Physiol.* **50**, 603-629.

Dent, J. A. and Avery, L. (1993). A defined medium for the pharynx. *Worm Breeder's Gazette* **13**, 44.

Dent, J. A., Davis, M. W. and Avery, L. (1997). avr-15 encodes a chloride channel subunit that mediates inhibitory glutamatergic neurotransmission and ivermectin sensitivity in Caenorhabditis elegans. *EMBO J.* **16**, 5867-5879.

DiFrancesco, D. (1993). Pacemaker mechanisms in cardiac tissue. *Annu. Rev. Physiol.* **55**, 455-472.

Doncaster, C. C. (1962). Nematode feeding mechanisms. I. Observations on *Rhabditis* and *Pelodera*. *Nematologica* **8**, 313-320.

Fleischhauer, R., Davis, M. W., Dzhura, I., Neely, A., Avery, L. and Joho, R. H. (2000). Ultrafast inactivation causes inward rectification in a voltage-gated K(+) channel from *Caenorhabditis elegans*. *J. Neurosci.* **20**, 511-520.

Francis, M. M., Mellem, J. E. and Maricq, A. V. (2003). Bridging the gap between genes and behavior: recent advances in the electrophysiological analysis of neural function in *Caenorhabditis elegans*. *Trends Neurosci.* **26**, 90-99.

Franks, C. J., Pemberton, D., Vinogradova, I., Cook, A., Walker, R. J. and Holden-Dye, L. (2002). Ionic basis of the resting membrane potential and action potential in the pharyngeal muscle of *Caenorhabditis elegans*. *J. Neurophysiol.* **87**, 954-961.

Gentet, L. J., Stuart, G. J. and Clements, J. D. (2000). Direct measurement of specific membrane capacitance in neurons. *Biophys. J.* **79**, 314-320.

Goodman, M. B., Hall, D. H., Avery, L. and Lockery, S. R. (1998). Active currents regulate sensitivity and dynamic range in *C. elegans* neurons. *Neuron* **20**, 763-772.

Hagiwara, N., Irisawa, H. and Kameyama, M. (1988). Contribution of two types of calcium currents to the pacemaker potentials of rabbit sino-atrial node cells. *J. Physiol. (Lond).* **395**, 233-253.

Hille, B. (2001). *Ion Channels of Excitable Membranes*. Sunderland, MA: Sinauer.

Jospin, M., Jacquemond, V., Mariol, M. C., Segalat, L. and Allard, B. (2002a). The L-type voltage-dependent Ca^{2+} channel EGL-19 controls body wall muscle function in *Caenorhabditis elegans*. *J. Cell Biol.* **159**, 337-348.

Jospin, M., Mariol, M. C., Segalat, L. and Allard, B. (2002b). Characterization of K(+) currents using an in situ patch clamp technique in body wall muscle cells from *Caenorhabditis elegans*. *J. Physiol.* **544**, 373-384.

Keane, J. and Avery, L. (2003). Mechanosensory inputs influence *Caenorhabditis elegans* pharyngeal activity *via* ivermectin sensitivity genes. *Genetics* **164**, 153-162.

Lee, J. H., Gomora, J. C., Cribbs, L. L. and Perez-Reyes, E. (1999). Nickel block of three cloned T-type calcium channels: low concentrations selectively block alpha1H. *Biophys. J.* **77**, 3034-3042.

Lee, R. Y., Lobel, L., Hengartner, M., Horvitz, H. R. and Avery, L. (1997). Mutations in the alpha1 subunit of an L-type voltage-activated Ca2+ channel cause myotonia in *Caenorhabditis elegans*. *EMBO J.* **16**, 6066-6076.

Maupas, E. (1900). Modes et formes de reproduction dés nematodes. *Arch. Zool. Exp. Genet.* **8**, 463-624.

McKay, J. P., Raizen, D. M., Gottschalk, A., Schafer, W. R. and Avery, L. (2004). eat-2 and eat-18 are required for nicotinic neurotransmission in the *Caenorhabditis elegans* pharynx. *Genetics* **166**, 161-169.

Mellem, J. E., Brockie, P. J., Zheng, Y., Madsen, D. M. and Maricq, A. V. (2002). Decoding of polymodal sensory stimuli by postsynaptic glutamate receptors in *C. elegans*. *Neuron* **36**, 933-944.

Pierce-Shimomura, J. T., Faumont, S., Gaston, M. R., Pearson, B. J. and Lockery, S. R. (2001). The homeobox gene lim-6 is required for distinct chemosensory representations in *C. elegan*s. *Nature* **410**, 694-698.

Raizen, D. M. and Avery, L. (1994). Electrical activity and behavior in the pharynx of *Caenorhabditis elegans*. *Neuron* **12**, 483-495.

Raizen, D. M., Lee, R. Y. and Avery, L. (1995). Interacting genes required for pharyngeal excitation by motor neuron MC in *Caenorhabditis elegans*. *Genetics* **141**, 1365-1382.

Richmond, J. E. and Jorgensen, E. M. (1999). One GABA and two acetylcholine receptors function at the *C. elegans* neuromuscular junction. *Nat. Neurosci.* **2**, 791-797.

Seymour, M. K., Wright, K. A. and Doncaster, C. C. (1983). The action of the anterior feeding apparatus of *Caenorhabditis elegans* (Nematoda: Rhabditida). *J. Zool. (Lond.)* **201**, 527-539.

Sherman-Gold, R. (1993). *The Axon Guide For Electrophysiology and Biophysics Laboratory Techniques*. Union City, CA: Axon Instruments, Inc.

Spector, P. S., Curran, M. E., Zou, A., Keating, M. T. and Sanguinetti, M. C. (1996). Fast inactivation causes rectification of the IKr channel. *J. Gen. Physiol.* **107**, 611-619.

Steger, K. A. (2003). Cholinergic regulation of feeding in *C. elegans*: studies of a T-type calcium channel and three muscarinic acetylcholine receptors. PhD dissertation, The University of Texas Southwestern Medical Center at Dallas.

Steger, K. A., Shtonda, B. B., Thacker, C., Snutch, T. P. and Avery, L. (2005). The *Caenorhabditis elegans* T-type calcium channel CCA-1 boosts neuromuscular transmission. *J. Exp. Biol.* **208**, 2191-2203.

Sulston, J. and Hodgkin, J. (1988). Methods. In *The Nematode* C. elegans (ed. Wood W), pp. 587-606. Cold Spring Harbor, NY: Cold Spring Harbor Laboratory Press.

Trent, C., Tsuing, N. and Horvitz, H. R. (1983). Egg-laying defective mutants of the nematode *Caenorhabditis elegans*. *Genetics* **104**, 619-647.

Wang, Z. W., Saifee, O., Nonet, M. L. and Salkoff, L. (2001). SLO-1 potassium channels control quantal content of neurotransmitter release at the *C. elegans* neuromuscular junction. *Neuron* **32**, 867-881.

Yuan, A., Dourado, M., Butler, A., Walton, N., Wei, A. and Salkoff, L. (2000). SLO-2, a K^+ channel with an unusual Cl^- dependence. *Nat. Neurosci.* **3**, 771-779.

Zheng, Y., Mellem, J. E., Brockie, P. J., Madsen, D. M. and Maricq, A. V. (2004). SOL-1 is a CUB-domain protein required for GLR-1 glutamate receptor function in *C. elegans*. *Nature* **427**, 451-457.